# Zuschriften

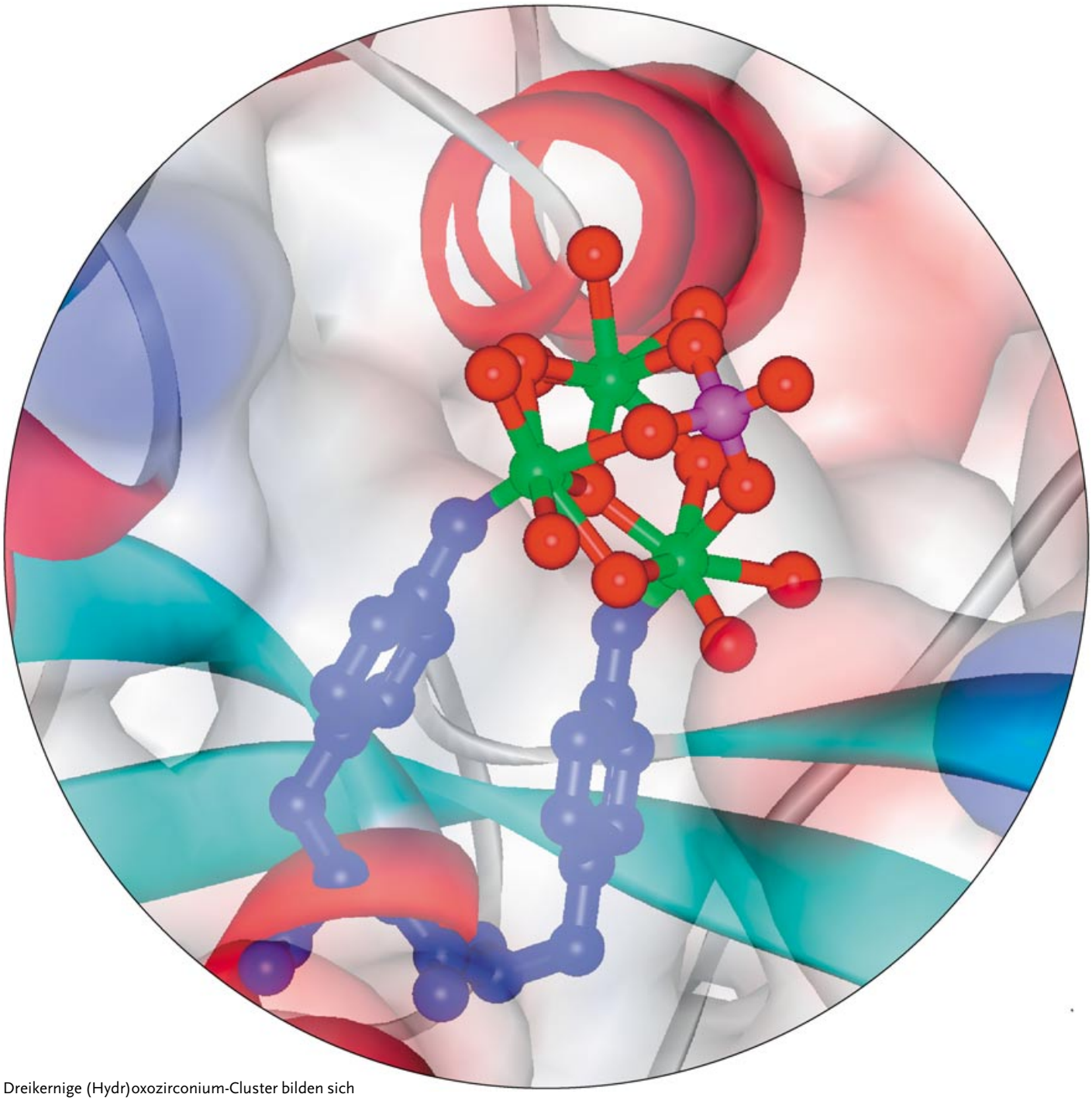

Dreikernige (Hydr)oxozirconium-Cluster bilden sich in der Venusfliegenfallen-artigen Interdomänenbindungstasche von bakteriellem Transferrin und sind dort über zwei Phenolatliganden benachbarter Tyrosinreste verankert. Die Cluster entstehen vermutlich durch schrittweise Insertion von $Zr^{IV}$-Ionen in die Tasche. Mehr darüber erfahren Sie in der Zuschrift von P. J. Sadler et al. auf den folgenden Seiten.


**DOI: 10.1002/ange.200460806**

*Bioinorganic Chemistry*

# Assembly of an Oxo–Zirconium(IV) Cluster in a Protein Cleft**

*Weiqing Zhong, Dmitriy Alexeev, Ian Harvey, Maolin Guo, Dominic J. B. Hunter, Haizhong Zhu, Dominic J. Campopiano, and Peter J. Sadler**

There is a wide range of potential uses for small, well-defined oxo–metal clusters, including magnetic devices, optical materials, and catalysts.[1] The challenge is to discover synthetic methods that allow their size, composition, and, importantly, also the external coating (peripheral ligands) to be controlled. These features determine the chemical and physical properties of the metals in the cluster, including recognition by interacting partners, such as substrates and surfaces. We are exploring the use of flexible protein clefts as templates for assembly of polyoxometalate clusters, in particular that of bacterial transferrin (ferric-ion-binding protein, Fbp). Recently we,[2,3] and others,[4] have shown that the "venus fly trap" interdomain cleft of Fbp can accommodate clusters of metal ions, which are effectively small fragments of oxo/hydroxo minerals. Herein we show that oxo–zirconium clusters are readily assembled on Fbp by reaction with a mononuclear $Zr^{IV}$ complex and nucleated by a dityrosyl (diphenolate) motif in the interdomain binding cleft. We have determined the structures of these multinuclear zirconium–Fbp adducts by EXAFS and X-ray crystallography, and have studied the influence of phosphate and carbonate on the assembly process.

Native, holo-Fbp (34 kDa, 309 amino acids) contains an $Fe^{III}$ center bound to the phenolate oxygen atoms of Tyr195 and Tyr196, a carboxylate oxygen atom of Glu57, and the imidazole nitrogen atom of His9, together with oxygen atoms from phosphate (the "synergistic anion") and water (Figure 1), in a closed binding cleft.[5] The cleft is formed by

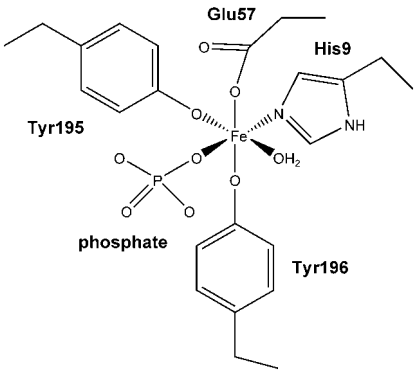


***Figure 1.*** The iron(III)-binding site in holo-Fbp.

two alternating α helix/β sheet domains hinged by a pair of antiparallel β strands. Serum transferrin and lactoferrin have similar $Fe^{III}$-binding sites, but use carbonate as the synergistic anion. Carbonate can replace phosphate in holo-Fbp, but binds less strongly.[6,7]

We prepared Zr–Fbp by treating apo-Fbp with various molar ratios of $[Zr(NTA)_2]^{2-}$ (NTA = *N*,*N*-bis(carboxymethyl) glycine, ion (3−)) in HEPES (HEPES = 2-(4-(2-hydroxyethyl)-1-piperazinyl)ethanesulfonic acid) buffer pH 7.4 for 24 h followed by extensive ultrafiltration to remove unbound $Zr^{IV}$. Reaction with 1, 2, and 6 mol equivalents of $[Zr(NTA)_2]^{2-}$ gave proteins containing an average of 0.8, 1.5, and 3.9 mol Zr, respectively, together with approximately 1 mol of phosphate per mol protein, as determined by inductively coupled plasma atomic emission spectroscopy (ICP-AES; Table 1). Similar results were obtained using Tris (Tris = 2-amino-2-(hydroxymethyl)-1,3-propanediol) buffer at pH 8 (Table 1). Chromatographic studies suggested that the products from these reloading reactions contain both apo and multinuclear forms of Zr–Fbp (see Supporting Information).

The presence of bound clusters was confirmed by Zr K-edge EXAFS studies. The products from 1:1 and 6:1 reactions of $[Zr(NTA)_2]^{2-}$ with apo-Fbp gave essentially the same EXAFS spectra (Figure 2), and clearly show the presence of Zr–Zr scattering between 3.3–3.6 Å, consistent with the presence of $\{Zr_3\}$ clusters in both preparations. The apparent slight difference in the distances observed in the Fourier

[*] Dr. W. Zhong, Dr. M. Guo,[++] Dr. D. J. B. Hunter, Dr. H. Zhu, Dr. D. J. Campopiano, Professor Dr. P. J. Sadler
School of Chemistry
King's Buildings
The University of Edinburgh
West Mains Road, Edinburgh EH9 3JJ (UK)
Fax: (+44) 131-650-6453
E-mail: p.j.sadler@ed.ac.uk
Dr. W. Zhong
School of Pharmacy
Second Military Medical University
Shanghai, 200433 (P. R. China)
Dr. D. Alexeev[+]
Institute of Cell and Molecular Biology
Michael Swann Building, University of Edinburgh
Mayfield Road, Edinburgh EH9 3JR (UK)
E-mail: Dmitriy-Alexeev@hotmail.com
Dr. I. Harvey
Synchrotron Radiation Department
CCLRC Daresbury Laboratory, Warrington WA4 4AD (UK)
[+] X-ray data. Current address:
Millennium Pharmaceuticals Ltd.
45 Sidney Street, Cambridge, MA 02139 (USA)
[++] Current address:
Department of Chemistry and Biochemistry
University of Massachusetts Dartmouth
285 Old Westport Road, North Dartmouth, MA 02747-2300 (USA)

[**] We thank The Wellcome Trust (Travelling Research Fellowship and International Research Development Award for WZ, Sir Henry Wellcome Commemorative Award for DJC and PJS, and Edinburgh Protein Interaction Centre), The Darwin Trust, CCLRC, EPSRC, Royal Society, Wolfson Foundation and the Medical Science Foundation of Chinese PLA (grant No. 01H021 for WZ) for their support for this work, and Dr Lorna Eades and John Wexler for assistance with ICP-MS and graphics, respectively.

Supporting information for this article is available on the WWW under http://www.angewandte.org or from the author.

  DOI: 10.1002/ange.200460806 

***Table 1:*** Analysis of the products from reactions of apo-Fbp with $[Zr(NTA)_2]^{2-}$.

| Reaction mixture[a] | Product[b] | |
|---|---|---|
| [Zr]/[Fbp] | [Zr]/[Fbp] | [P]/[Fbp] |
| 1:1[c] | 0.84 | –[d] |
| 2:1[e] | 1.5 | 1.4 |
| 6:1[e] | 3.9 | 1.1 |

[a] Reactions carried out for 24 h in 10 mM HEPES buffer containing 5 mM phosphate and 5 mM carbonate, pH 7.4, 298 K. [b] Fbp concentration determined from $A_{280}$. [c] Similar analyses obtained for reactions in 10 mM phosphate and carbonate. [d] Not determined. [e] Similar analyses obtained for reactions in 10 mM Tris buffer pH 8.0.

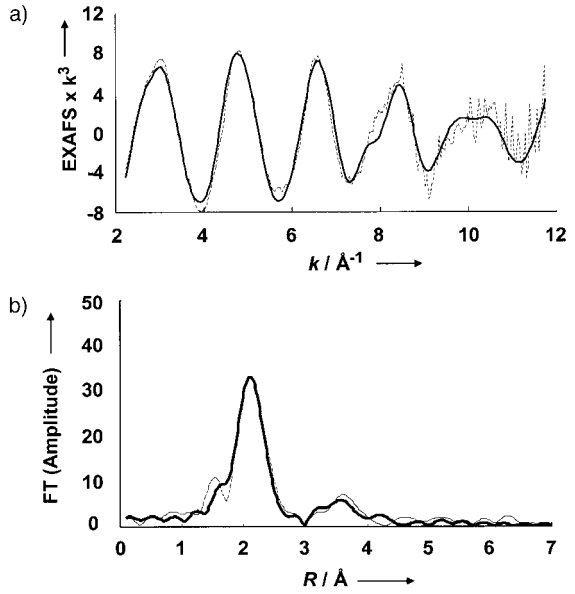


***Figure 2.*** a) EXAFS data, and b) and the Fourier transform data for Zr–Fbp (prepared from 6:1 Zr:apo-Fbp reaction). The data are modeled using the cluster derived from the X-ray data (see Figure 3) but with carbonate as the capping ligand, and full multiple scattering (see Supporting Information for details). Dashed line = experimental data, bold line = model. The peak at approximately 1.5 Å in (b) is an artifact of background subtraction and Fourier truncation (finite EXAFS data range).

transforms for the two samples (see Supporting Information) reflects small differences in the geometry of the clusters (as is also seen in the crystallographic data, see below). The EXAFS data represent an average of the $\{Zr_3\}$ local environments and could also reflect a higher Zr loading at some centers. The first shell can be fitted with 1 oxygen atom at approximately 2.0 Å, 4 oxygen atoms at approximately 2.15 Å, and a further 2 oxygen atoms at approximately 2.3 Å (see Table 2). However, this leaves an unfilled contribution to the first shell at approximately 2.66 Å. This contribution can be fitted with a carbon atom, which reduces the *R* factor by 6%. A light atom at this distance is consistent with bound carbonate, rather than phosphate. Indeed, inclusion of carbonate rather than phosphate in the final EXAFS model leads to significantly lower *R* factors (29.1% versus 36.5% for 1:1, 25.0% versus 32.2% for the product from the 6:1 reaction) as well as much better matches to the Fourier

***Table 2:*** Refined average EXAFS interatomic distances from the Zr "central atom", modeled with carbonate as a capping ligand, including multiple scattering.

| Atoms/parameter | Sample[a] | |
|---|---|---|
| | Zr–Fbp (1:1) | Zr–Fbp (6:1) |
| 1 O [Å] | 2.03(±0.02) | 1.99(±0.02) |
| 4 O [Å] | 2.16(±0.02) | 2.13(±0.01) |
| 2 O [Å] | 2.30(±0.02) | 2.27(±0.01) |
| 1 Zr [Å] | 3.41(±0.02) | 3.38(±0.02) |
| 1 Zr [Å] | 3.53(±0.03) | 3.50(±0.02) |
| *R* factor [%] | 29.1 | 25.0 |
| fit index | 0.535 | 0.437 |

[a] Ratios refer to the reaction stoichiometry.

transforms (see Figure 2). However, owing to the strength of the Zr–Zr scattering and the averaging of the EXAFS data over three zirconium atoms per cluster, a proportion of clusters with bound phosphate cannot be ruled out. Evidence that carbonate can bind to Zr–Fbp in solution was obtained by NMR spectroscopy. The $^{13}C$-{$^1H$} NMR spectrum of apo-Fbp (0.4 mM) in the presence of 2 mol equivalents of $[Zr(NTA)_2]^{2-}$ and 20 mM $NaH^{13}CO_3$ contained a small resonance signal at $\delta = 168.2$ ppm assignable to zirconium-bound $[^{13}CO_3]^{2-}$ (see Supporting Information).[8]

Crystallization of Zr–Fbp was successful only using a malate/imidazole buffer system and a slightly higher pH value (8–8.2). Crystals were grown at 290 K by the hanging-drop vapor-diffusion technique, using Zr–Fbp obtained by reaction of apo-Fbp with either 1, 4, or 6 mol equivalents of $Zr^{IV}$, again after ultrafiltration to remove unbound metal. These preparations all gave similar crystals, which contain nine independent molecules in the asymmetric unit. In the 1.5 Å resolution structure (Table 3), all the molecules contain $\{Zr_3\}$ clusters, with minor differences in bond lengths and angles. The interdomain binding cleft remains open and Zr1 and Zr3 are coordinated directly to Tyr195 and Tyr196, respectively, and to a capping anion which appeared to be best modeled as phosphate, Figure 3 (and Supporting Information). The

***Table 3:*** Crystallographic data and refinement statistics.

| Parameter | $Zr_3$–Fbp[a] |
|---|---|
| wavelength [Å] | 0.978 |
| resolution [Å] | 20–1.5 |
| refined twinning fraction [%] | 49.0 |
| completeness [%] | 98.5 (94.1) |
| redundancy | 4.9 (2.9) |
| $I/\Sigma$ | 16.3 (1.3) |
| $R_{sym}$[b] [%] | 9.5 (80.9) |
| $R_{cryst}$[c] [%]/$R_{free}$[d] [%] | 19.2/27.5 |
| rms deviations | |
| bonds [Å] | 0.01 |
| angles [°] | 2.3 |
| average B-factors | |
| protein [Å$^2$] | 25.5 |
| water [Å$^2$] | 27.6 |

[a] Numbers in parentheses are for the highest resolution shell. [b] $R_{sym} = \Sigma|I_h - \langle I_h\rangle|/I_h$, where $\langle I_h\rangle$ is the average intensity over symmetry equivalent reflections. [c] $R_{cryst} = \Sigma|F_o - F_c|/\Sigma F_o$, where summation is over the data used for refinement. [d] $R_{free}$ was calculated using 5% of data excluded from refinement.

  

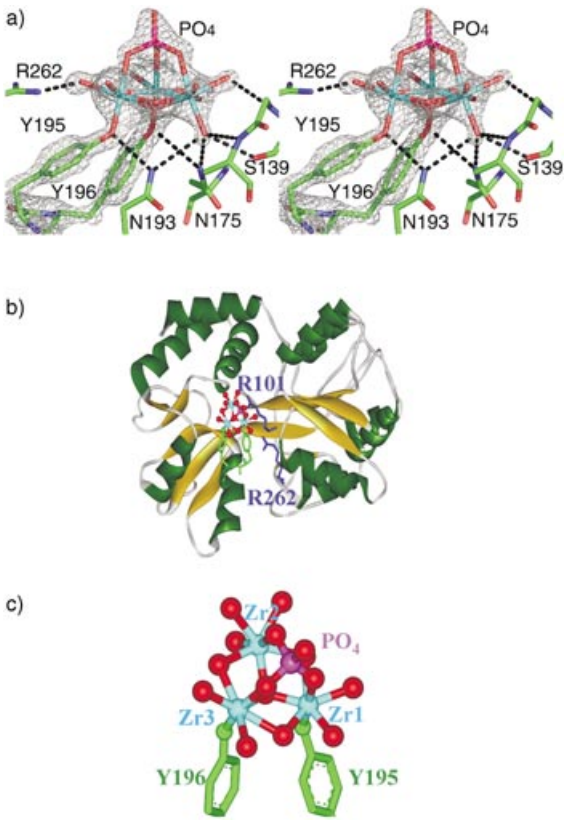


***Figure 3.*** The crystal structure of $Zr_3$–Fbp. a) Stereo pair of the electron density map (contoured at the 3.5σ level) of the oxo–$Zr_3$ phosphate cluster (Zr cyan). The map was averaged between all nine molecules in the asymmetric unit. Only the electron density around Tyr195, Tyr196 and the cluster is shown. The only direct coordination to the $Zr^{IV}$ ions in the cluster is by Tyr195 and Tyr196, although the oxygen atoms of the oxo cluster are H-bonded to several amino acids including residues 139–141 on the right side of the cluster in the phosphate-binding loop. b) Ribbon diagram of the protein (molecule D) showing α helices (dark green), β sheets (gold), and the {$Zr_3$} cluster in the interdomain cleft. Residue and atom colors: Tyr195 and Tyr196 green, Arg101 and Arg262 blue, P (phosphate) pink, oxygen red, Zr cyan. c) The anchoring of the trinuclear cluster by the dityrosyl motif, showing Zr labelling.

cluster structure resembles those found in the oxo–zirconium methacrylate clusters, $[Zr_6(OH)_4O_4(OMc)_{12}]$ and $[Zr_4O_2(OMc)_{12}]$ (OMc = methacrylate),[9] and in the oxo–zirconium biphenolate cluster $[(L_2Zr)_3(OH)_3(O)\text{-}Li_5(thf)_8(H_2O)_5]$ (L = 2,2′-biphenolato dianion),[10] and is based on a triangular $Zr_3O_4$ unit with a central bridging $\mu_3$-oxygen atom and three bridging $\mu_2$-oxygen atoms. Each zirconium atom in $Zr_3$–Fbp is bound to seven oxygen atoms (in agreement with the EXAFS data) in a pentagonal bipyramidal geometry. The five equatorial oxygen atoms are (hydr)oxides, and the axial oxygen atoms are from tyrosinate for Zr1 and Zr3, water for Zr2, and from phosphate (Figure 3c). The Zr···Zr separations range from 3.4 to 3.7 Å, and the Zr–O bond lengths from 2.1–2.4 Å, with the zirconium–tyrosinate bonds being the shortest (1.9–2.1 Å). The positively charged side-chains of Arg101 (which is fully conserved in bacterial transferrins[3]) and Arg262 are hydrogen-bonded to oxygen atoms of the oxo–$Zr_3$ cluster, as are the side-chains or main chain NH groups of several other amino acids including S139, N175, and N193 (see Figure 3a). The relatively high homogeneity of the zirconium clusters can be contrasted with the heterogeneity of the clusters in Hf-Fbp which were tri- and pentanuclear, either with or without capping phosphate.[2]

We studied reactions of apo-Fbp (14 μM) with $[Zr(NTA)_2]^{2-}$ in 10 mM HEPES buffer containing 5 mM $NaHCO_3$, 5 mM phosphate, pH 7.4, 298 K, by UV/Vis spectroscopy. Two new peaks appeared in the difference spectrum at 247 nm and 295 nm (Figure 4a,b). These bands are assignable to π–π transitions of Tyr residues deprotonated by binding to $Zr^{IV}$. Similar bands are seen when both bacterial and serum transferrins bind to a wide variety of metal ions.[8,11,12] Titration studies (Figure 4c,d) suggested that a zirconium:protein mol ratio of 1:1 is sufficient to deprotonate both Tyr195 and Tyr196 if phosphate is present as the synergistic anion, but only one Tyr residue when only (bi)carbonate is present (Figure 4b). Phosphate is known to bind in the interdomain cleft of the apo protein and may prepare the cleft for metal entry.[13] Beyond a 1:1 $[Zr(NTA)_2]^{2-}$:apo-Fbp ratio there was little increase in the absorption at 247 nm (Figure 4d). These data therefore suggest that the initial reaction with apo-Fbp involves $Zr^{IV}$ binding to Tyr195 and Tyr196 followed by subsequent formation of (hydr)oxo–zirconium clusters, and hence little increase in the absorption at 247 nm beyond a 1:1 $[Zr(NTA)_2]^{2-}$:apo-Fbp ratio. Thus the clusters appear to be formed by stepwise insertion of $Zr^{IV}$ ions into the interdomain cleft. ESI-MS studies of $K_2[Zr(NTA)_2]\cdot 2H_2O$ (5 mM) in aqueous solution and HEPES buffer gave a major peak at $m/z$ 582.88 (calcd. 582.82 for $\{K_3Zr(NTA)_2\}^+$}, with appropriate isotope splitting pattern, showing that the complex is monomeric under the conditions used for MS (50 % $CH_3CN$/$H_2O$, 0.1 % formic acid). The mobility of Tyr196 (as observed in crystals of oxo–$Fe^{III}$–Fbp)[3] in particular may be important for capturing $Zr^{IV}$ ions at the protein surface and delivering them into the binding cleft. The possibility that the protein can also capture preformed oxo–tri-$Zr^{IV}$ clusters cannot be ruled out.

Low-molecular-weight alkoxide and aryloxide ligands have been used in the synthesis of small organically functionalized oxo–$Zr^{IV}$ clusters.[1,14–17] The experiments described herein show that oxo–trizirconium clusters anchored by a dityrosyl (diphenolate) motif readily assemble in the hinged cleft of a protein, bacterial transferrin. The provision of a protein coat for a polyoxometalate cluster could have several advantages. For example, the protein can readily be engineered to allow the environment of the cluster to be modified, including the electrostatic potential and hydrophobicity of the outer coordination sphere. Also the amino acids on the protein surface can be mutated to facilitate attachment to other surfaces (e.g. for array experiments), or to promote solubilization in various media. It is apparent that Fbp is a versatile metal-binding scaffold. The remarkable ability of the dityrosyl motif to selectively nucleate the formation of oxo–metal clusters in a positively charged binding cleft is likely to be a useful and widely exploitable property of the protein.

  

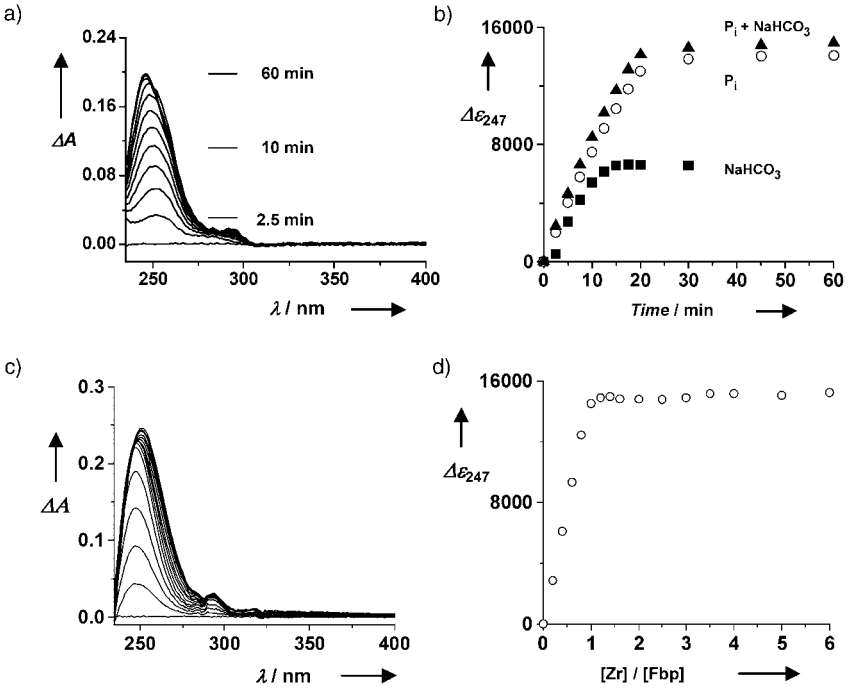


***Figure 4.*** a) Difference UV/Vis spectra recorded at various times during the reaction of apo-Fbp (14 μM) with 2.0 mol equivalents of $[Zr(NTA)_2]^{2-}$ in 10 mM HEPES pH 7.4 in the presence of 5 mM $NaHCO_3$ and 5 mM $KH_2PO_4$. b) Plot of molar absorptivity versus time for reaction in the presence of 5 mM $NaHCO_3$ and 5 mM $KH_2PO_4$ (▲), and for similar reactions with either 5 mM $NaHCO_3$ (■) or 5 mM of $KH_2PO_4$ (○) present. c) Difference UV/Vis spectra for the titration of apo-Fbp (15 μM) with $[Zr(NTA)_2]^{2-}$ in 10 mM HEPES, 5 mM $NaHCO_3$, pH 7.4, 298 K (1 h equilibration). Mol ratios of $[Zr(NTA)_2]^{2-}$: apo-Fbp from bottom to top: 0–1.6 in 0.2 mol equivalent steps, then 2.0, 2.5, 3.0, 3.5, 4.0, 5.0, 6.0. d) Titration curve for the reaction in (c).

## Experimental Section

HEPES, $H_3NTA$, and Fe and Zr atomic absorption standard solutions were purchased from Aldrich, $NaH^{13}CO_3$ (>99% enriched) from MSD isotopes, and $ZrOCl_2$ hydrate from Strem Chemicals (Zr content determined by ICP-AES). Crystalline $K_2[Zr(NTA)_2]\cdot 2H_2O$ was prepared according to a literature method.[8,18] Holo- and apo-Fbp were prepared and purified by modifications of described methods.[6,19]

Zr–Fbp: Typically, microlitre aliquots of $NaHCO_3$ (0.25 M) and $KH_2PO_4$ (0.25 M, pH 7.4, final concentrations 5 mM) were added to apo-Fbp (25–100 μM) in 10 mM HEPES buffer pH 7.4 (or Tris buffer pH 8.0), followed by addition of freshly prepared aqueous $K_2[Zr(NTA)_2]$ (10 mM) to give ratios of [Zr]:[Fbp] = 1:1, 2:1, 4:1, or 6:1. The mixture was incubated for 24 h at 310 K, and the buffer was exchanged into 0.1 M KCl by ultrafiltration 8× (to remove unbound Zr, carbonate, and phosphate) and the solution was concentrated to approximately 8 mg protein $mL^{-1}$.

Crystals were grown by the hanging-drop vapor-diffusion technique at 290 K by mixing protein solution (5 μL; 3.7–4.0 mg $mL^{-1}$ in 0.1 M KCl) with an equal amount of a reservoir solution containing approximately 20–22% polyethylene glycol (PEG) 4000, 0.2 M NaCl, 0.4 M imidazole/malate buffer, pH 8.0–8.2.

Crystals were flash-frozen in liquid nitrogen and X-ray data were collected on station 14.2 (SRS, Daresbury Laboratory; $\lambda = 0.978$ Å) using an ADSC Quantum4 CCD detector and processed and scaled using HKL2000.[20] Crystals belong to the space group $P3_2$ (cell dimensions $a = b = 146.2$ Å and $c = 113.56$ Å). The structures were solved using the methods previously described.[2]

Coordinates have been deposited in the Protein Data Bank (accession code 1XC1).

**X**-ray spectra were recorded at the Zr K-edge on EXAFS station 9.3 at Daresbury Laboratory Synchrotron Radiation Source (operating at 2 GeV), at 80 K, and in fluorescence mode. Data collection times were 11 h per sample.

A computer-controlled Perkin-Elmer Lambda 16 UV/Vis spectrometer was used together with 1 cm path-length cuvettes maintained at 298 ± 0.1 K or 310 ± 0.1 K with a PTP-1 Peltier temperature programmer. Aliquots (2 or 5 μL) of a $[Zr(NTA)_2]^{2-}$ solution were added to apo-Fbp (10–20 μM) solutions in HEPES buffer (10 mM), and $NaHCO_3$ (5 mM) and left to equilibrate for 1 h at 298 K or 310 K. The UV/Vis spectra were then recorded. A buffer solution containing the same amounts of $NaHCO_3$ and $[Zr(NTA)_2]^{2-}$ was used as the reference.

The time courses for the reactions of apo-Fbp with $[Zr(NTA)_2]^{2-}$ were also recorded in HEPES buffer (10 mM). Apo-Fbp (13–15 μM) in HEPES buffer (10 mM, pH 7.4) containing $NaHCO_3$ (5 mM) and/or $KH_2PO_4$ was treated with $[Zr(NTA)_2]^{2-}$ (2 mol equivalents) at 298 K and UV/Vis spectra were recorded at 2.5 min intervals against the same buffer solution containing the same amount of $[Zr(NTA)_2]^{2-}$.

The products from reaction of apo-Fbp (180 μM) with 0.5, 1.0 and 6.0 mol equiv of $[Zr(NTA)_2]^{2-}$ at 310 K for 24 h were applied to a Mono S HR5/5 column equilibrated with HEPES buffer (10 mM; pH 7.4, 25 mL), followed by gradient elution with 0–1 M KCl in HEPES (10 mM; pH 7.4) flow rate 0.5 mL $min^{-1}$). Fractions of 0.5 mL were collected and analyzed by ICP-AES, and of 0.1 mL by inductively coupled plasma (ICP)-MS.

Zr and P content was determined by ICP-AES (Thermo Jarrell Ash IRIS spectrometer) calibrated with standard solutions using the emission lines at 349.621 nm and 213.618 nm for Zr and P, respectively. For some samples, $^{90}Zr$ was determined on a PlasmaQuad ICP-MS. Samples from reactions of apo-Fbp with $[Zr(NTA)_2]^{2-}$ (Table 1) were purified by ultrafiltration (Centricon MW cut-off 10 kDa), washing 3× with HEPES or Tris buffer as appropriate before Zr and P analysis.

Details of ESI-MS, NMR, chromatography and pH measurements, and further details of protein preparation, X-ray crystallography and X-ray absorption spectroscopy are given in the Supporting Information.

Received: May 27, 2004
Published Online: October 7, 2004

**Keywords:** bioinorganic chemistry · cluster compounds · metalloproteins · X-ray diffraction · zirconium

[1] G. Kickelbick, D. Holzinger, C. Brick, G. Trimmel, E. Moons, *Chem. Mater.* **2002**, *14*, 4382–4389.
[2] D. Alexeev, H. Zhu, M. Guo, W. Zhong, D. J. B. Hunter, W. Yang, D. J. Campopiano, P. J. Sadler, *Nat. Struct. Biol.* **2003**, *10*, 297–302.

  

[3] H. Zhu, D. Alexeev, D. J. B. Hunter, D. J. Campopiano, P. J. Sadler, *Biochem. J.* **2003**, *376*, 35 – 41.
[4] S. R. Shouldice, R. J. Skene, D. R. Dougan, D. E. McRee, L. W. Tari, A. B. Schryvers, *Biochemistry* **2003**, *42*, 11908 – 11914.
[5] C. M. Bruns, A. J. Nowalk, A. S. Arvai, M. A. McTigue, K. G. Vaughan, T. A. Mietzner, D. E. McRee, *Nat. Struct. Biol.* **1997**, *4*, 919 – 924.
[6] M. Guo, I. Harvey, W. Yang, L. Coghill, D. J. Campopiano, J. A. Parkinson, R. T. A. MacGillivray, W. R. Harris, P. J. Sadler, *J. Biol. Chem.* **2003**, *278*, 2490 – 2502.
[7] S. Dhungana, C. H. Taboy, D. S. Anderson, K. G. Vaughan, P. Aisen, T. A. Mietzner, A. L. Crumbliss, *Proc. Natl. Acad. Sci. USA* **2003**, *100*, 3659 – 3664.
[8] W. Q. Zhong, J. A. Parkinson, M. L. Guo, P. J. Sadler, *J. Biol. Inorg. Chem.* **2002**, *7*, 589 – 599.
[9] G. Kickelbick, U. Schubert, *Chem. Ber.* **1997**, *130*, 473 – 477.
[10] D. Walther, B. Ritter, H. Gorls, G. Zahn, *Z. Anorg. Allg. Chem.* **1997**, *623*, 1125 – 1130.
[11] E. N. Baker, *Adv. Inorg. Chem.* **1994**, *41*, 389 – 463.
[12] H. Sun, H. Li, P. J. Sadler, *Chem. Rev.* **1999**, *99*, 2817 – 2842.
[13] C. M. Bruns, D. S. Anderson, K. G. Vaughan, P. A. Williams, A. J. Nowalk, D. E. McRee, T. A. Mietzner, *Biochemistry* **2001**, *40*, 15631 – 15637.
[14] W. J. Evans, M. A. Ansari, J. W. Ziller, *Polyhedron* **1998**, *17*, 869 – 877.
[15] Z. A. Starikova, E. P. Turevskaya, N. I. Kozlova, N. Ya Turova, D. V. Berdyev, A. I. Yanovsky, *Polyhedron* **1999**, *18*, 941 – 947.
[16] M. A. Walters, K.-C. Lam, S. Damo, R. D. Sommer, A. L. Reingold, *Inorg. Chem. Commun.* **2000**, *3*, 316 – 318.
[17] P. Sobota, S. Przybylak, J. Utko, L. B. Jerzykiewcz, *Organometallics* **2002**, *21*, 3497 – 3499.
[18] E. M. Larsen, A. C. Adams, *Inorg. Synth.* **1967**, *10*, 7 – 8.
[19] S. A. Berish, C. Y. Chen, T. A. Mietzner, S. A. Morse, *Mol. Microbiol.* **1992**, *6*, 2607 – 2615.
[20] Z. Otwinowski, W. Minor, *Methods Enzymol.* **1997**, *276*, 307 – 326.

  